Moisture transport in porous building materials

L. Pel, K. Kopinga
Eindhoven University of Technology, Department of Physics

H. Brocken
Eindhoven University of Technology, Department of Architecture and Building Technology

The isothermal moisture transport in various porous building materials during absorption and drying was studied by nuclear magnetic resonance (NMR). It is shown that the moisture diffusivity can be determined directly from measured transient moisture profiles. NMR appears to be an accurate and reliable method to determine these moisture profiles. For both water absorption and drying it is found that, within the experimental accuracy, a single unambiguous relation exists between the moisture diffusivity and the moisture content, which is dependent on the type of material. Preliminary absorption measurements on brick/mortar samples suggest that the hydraulic contact between mortar and brick may not be perfect.

Keywords: **moisture transport, moisture diffusivity, nuclear magnetic resonance, drying, absorption, brick/mortar interface.**

1 Introduction

Moisture in porous building materials can give rise to several kinds of damages, e.g., frost damage, salt crystallisation (Amoroso and Fassina, 1983), and mould growth (Adan, 1994). Therefore detailed knowledge of the moisture transport is essential for understanding the durability of these materials.

The mathematical formulation of mass transfer at the macroscopic level in porous media is usually based on diffusion equations. These were first established by Philip and de Vries (1957). Later, a more fundamental basis for these equations was given by Whitaker (1977) and Bear and Bachmat (1990). If gravity is neglected, the moisture transport for the one-dimensional isothermal problems that will be considered here can be described by a non-linear diffusion equation:

$$\frac{\partial \theta}{\partial t} = \frac{\partial}{\partial x}\left(D_\theta \frac{\partial \theta}{\partial x}\right) \tag{1}$$

In this equation θ [m^3m^{-3}] is the volumetric moisture content and D_θ [m^2s^{-1}] the moisture diffusivity. In this diffusion model all mechanisms for moisture transport, i.e., liquid flow and vapour

diffusion, are combined into a single moisture diffusivity, which is dependent on the actual moisture content.
The moisture diffusivity D_θ has to be determined experimentally for the porous medium of interest. By measuring the transient moisture profiles during the various transport processes, i.e., drying and absorption, the diffusion coefficient can be determined directly. These profiles were measured using a nuclear magnetic resonance (NMR) apparatus that was especially developed to study the moisture transport in porous building materials. We will present some typical results for soft-mud machine moulded fired-clay brick, mortar, and sand-lime brick, that were obtained during wetting as well as drying. All experiments discussed here were performed at an ambient temperature of 293 ± 0.5 K.

2 Nuclear magnetic resonance

In a nuclear magnetic resonance (NMR) experiment the magnetic moments of the hydrogen nuclei are manipulated by suitably chosen alternating radio frequency fields, resulting in a so-called spin-echo signal. The amplitude of this signal is proportional to the number of nuclei excited by the radio frequency field. NMR is a magnetic resonance technique, where the resonance condition for the nuclei is given by: $f = \gamma B_0$. Here f is the frequency of the alternating field, γ is the gyromagnetic ratio ($\gamma = 42.58$ MHz$/T$ for ^1H) and B_0 is the externally applied static magnetic field. Because of the resonance condition the method can be made sensitive to only hydrogen and therefore to water, in contrast to attenuation methods (Dixon and Ekstrand, 1982).
The experiments described here were performed using a NMR apparatus that was designed such that quantitative measurements of the moisture profile can be performed (unlike standard MRI (Magnetic Resonance Imaging), which is generally used in a qualitative way). An extensive description of this apparatus can be found in Kopinga *et al.* (1994) and Pel (1995).
The samples used in these measurements are cylinders with a diameter of 20 mm and a length ranging between 25 and 180 mm. The one-dimensional resolution of the NMR apparatus is about 1.0 mm, whereas the moisture content at a certain position in these samples can be determined with an inaccuracy of 1% within 40 s. During the measurements of a moisture profile a time stamp is added to each point of that profile, in order to enable a comparison with appropriate theoretical predictions.

3 Water absorption

In the absorption experiments cylindrical samples of initially dry material were allowed to freely absorb water through one end. At the start of a measurement, the lower end of the sample was inserted in a small water reservoir to about 1 mm below the water surface. The resulting moisture profiles, each measured at a different time, are given in Fig. 1 for one type of fired-clay brick. As can be seen from the figure a very steep wetting front is formed.

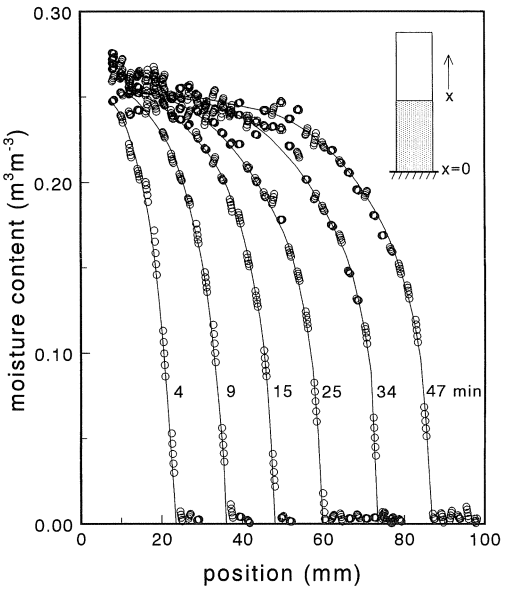

Fig. 1. Moisture profiles measured during the absorption of water in a fired-clay brick (RZ). The curves are only meant as a guide to the eye, whereas the times are only given as an indication of the elapsed time. In the inset a sketch of the experimental configuration is given.

If equation 1 is valid, all experimental profiles of one type of material can be related by the Boltzmann transformation, $\lambda = x\, t^{-1/2}$. The transformed moisture profiles for various materials are plotted in Fig. 2 as a function of λ. For all materials the Boltzmann transformation indeed yields distinct curves, on which the data from the various profiles collapse for the individual materials. To determine the dependence of D_θ on the moisture content, we use the well-known solution of equation 1 after the Boltzmann transformation:

$$D_\theta = -\frac{1}{2}\frac{1}{\left(\frac{d\theta}{d\lambda}\right)_\theta}\int_{\theta_0}^{\theta}\lambda\, d\theta' \qquad (2)$$

Using this equation, D_θ can be calculated numerically from the transformed experimental moisture profiles. Typical results for various building materials are presented in Fig. 3. The data show some scatter, which originates from the calculation of the numerical derivative in the evaluation of equation 2.

The behaviour of D_θ describing the liquid transport is commonly approximated by an exponential function: $D_\theta = D_{\theta,0}\exp(\beta\theta)$. In principle, the sets of data presented in Fig. 3 may be fitted with such an exponential function. However, the coefficients $D_{\theta,0}$ and β determined from such fits were found to be rather inaccurate. Therefore, the coefficients were varied within the error bounds given by the fitting procedure in such a way, that the best description of the corresponding data in Fig. 2 was obtained. For this purpose computer simulations of the moisture transport were used.

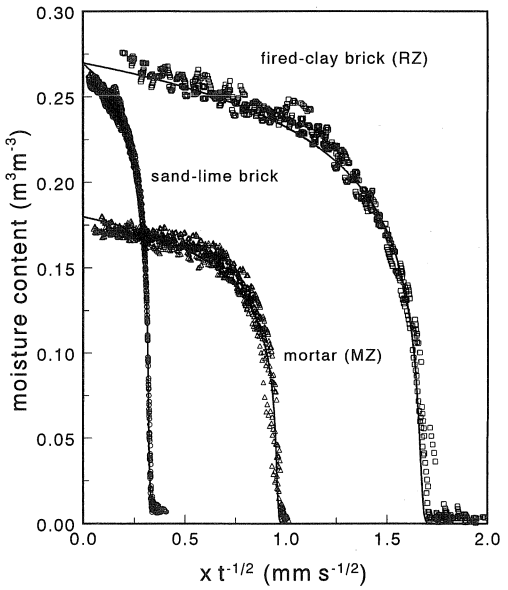

Fig. 2. (□, △, ○) *Boltzmann transformation of the measured moisture profiles for the various building materials.* (–) *Boltzmann transformation of simulated moisture profiles based on an exponential moisture diffusivity:* $D_\theta = D_{\theta,0}\, exp(\beta\theta)$.

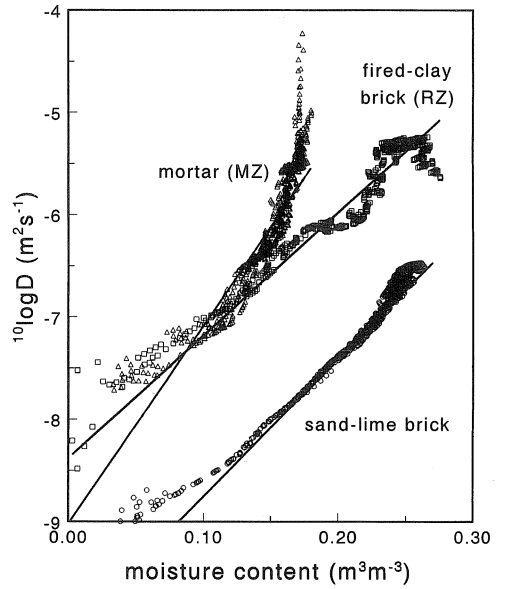

Fig. 3. (□, △, ○) *Moisture diffusivity for absorption calculated by equation 2.* (–) *Exponential behaviour of the moisture diffusivity determined by comparing simulated profiles and the corresponding data.*

The results of these simulations are represented by the full curves in Fig. 2; the corresponding exponential functions for these materials are represented by the straight lines in Fig. 3. In all cases the computer simulation based on an exponential behaviour of the moisture diffusivity gives an adequate description of the observed moisture profiles.

4 Drying

Each drying experiment was performed for a period of 40 hours or longer by flowing air of 45% relative humidity across one face of a sample. The resulting moisture profiles for the various materials are plotted in Fig. 4a & b. Inspection of the profiles shows variations, which are substantially larger than the experimental noise, and reproduce from profile to profile, e.g., for fired-clay brick at a position of 5 mm. These variations reflect the inhomogeneities of the sample.

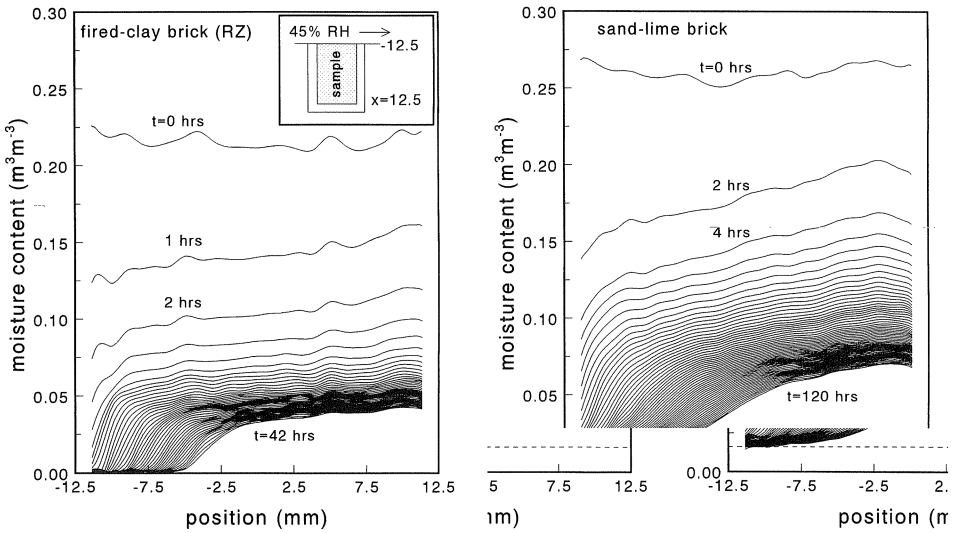

Fig. 4. Moisture profiles measured during drying of a fired-clay brick (RZ) and sand-lime brick. The time between subsequent profiles for the fired-clay brick is 1 hour and the profiles are given for a period of 42 hours. The time between subsequent profiles for the sand-lime brick is 2 hours and the profiles are given for a period of 120 hours. The dashed line indicates the residual moisture content observed at 45% relative humidity in this drying experiment. In the inset the experimental set-up is given.

In both cases a receding drying front is observed after some time. The evolution of the moisture profiles, however, is quite different for these two materials. For fired-clay brick a drying front is observed after approximately 7 hours, whereas it takes more than 20 hours for a drying front to develop in sand-lime brick. After the drying front has entered the material, a residual non-zero moisture content is observed for sand-lime brick.

As soon as drying has started, heat will be extracted and the temperature of the top of the sample will decrease. When the receding drying front enters the material, the drying is internally limited by vapour transport and hence the drying rate and thus the heat extracted from the sample are strongly decreased. About two hours later, i.e., about 8 hours after the start, the experiment can be regarded as isothermal (Pel, 1995).
To derive the D_θ from the experimental moisture profiles, equation 1 is integrated with respect to x, yielding::

$$D_\theta = \frac{\int_1^{x'} \left(\frac{\partial \theta}{\partial t}\right) dx}{\left(\frac{\partial \theta}{\partial x}\right)_{x'}} \qquad (3)$$

In this equation, use is made of the fact that the partial derivative of θ with respect to x is zero at the vapour tight bottom ($x = l$). The resulting numerically calculated moisture diffusivities are plotted against the corresponding moisture content in Fig. 5a & b. It is obvious, that the data in the figure have a significant scatter, which is rather pronounced at both high and low moisture contents. Nevertheless the data clearly reveal a well defined variation of the moisture diffusivity with moisture content.

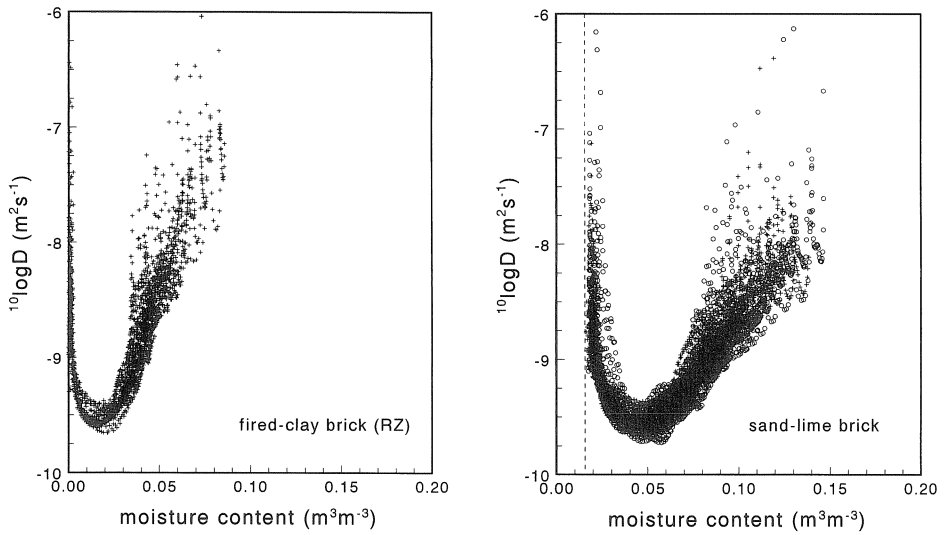

Fig. 5. (+, ○) Moisture diffusivity determined from the measured moisture profiles (see Fig. 4) plotted against the corresponding moisture content. The dashed line indicates the residual moisture content of sand-lime brick observed at 45% relative humidity in the drying experiments. Each figure contains over 2000 data points.

From error analysis it was shown that the grid for scanning and the one-dimensional resolution had only a minor influence on the determination of the moisture diffusivity for drying. The error in the calculation of the moisture diffusivity was dominated by experimental noise and inhomogeneities in the porosity of the material (Pel, 1995).

In order to simulate the drying of the materials under investigation, it is very important to determine the moisture diffusivity at low moisture contents correctly. In this regime the moisture transport is dominated by vapour transport, which limits the overall drying rate. However, the experimental results in Fig. 5 reveal that the moisture diffusivity in this range cannot be determined from the measured profiles with sufficient accuracy. Therefore we developed a new method of analysis based on the observed receding drying front. The velocity at which this front progresses into the material can be used to approximate the moisture diffusivity at low moisture contents: this diffusivity is approximated such that the receding drying front obtained from a computer simulation has the same front velocity as the experimentally determined one. This procedure is explained in more detail in Pel (1995). To determine the velocity, the position of the front has to be identified as a function of time. The moisture content at the minimum of the moisture diffusivity (roughly corresponding to the maximum of $\partial\theta/\partial x$, cf. Eq. 3) was chosen as a marker for the receding front position. In Fig. 6 the position of the front is plotted against time for the two materials given in Fig. 4. In both cases the receding front appears to have an almost constant velocity, in contrast to an often assumed $t^{-1/2}$ behaviour (Tammes and Vos, 1984).

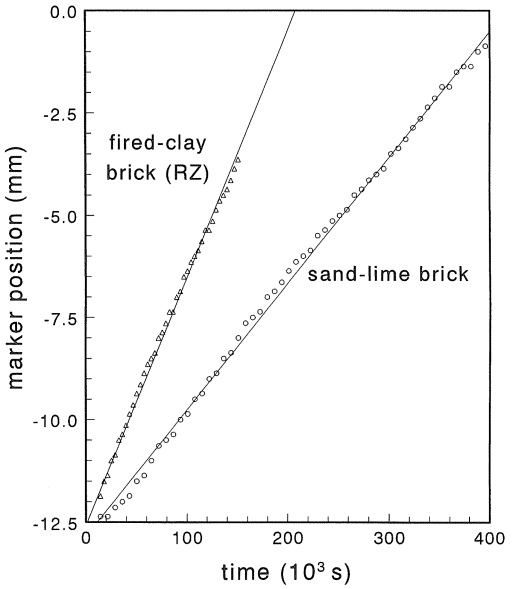

Fig. 6 Position of the marker indicating the receding drying front plotted against the time. The observed linear time dependence indicates that the front enters the material with a constant velocity.

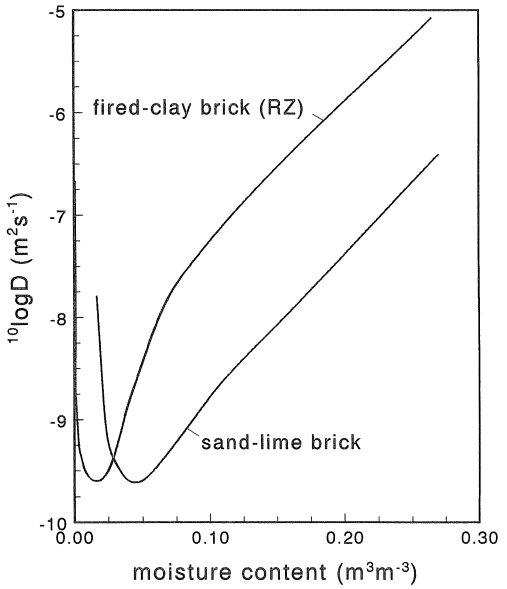

Fig. 7. Moisture diffusivity for drying over the full moisture content ran[illegible] by combining the moisture diffusivities determined from, successively, moisture profil[illegible] during absorption, during drying, and the receding front method.

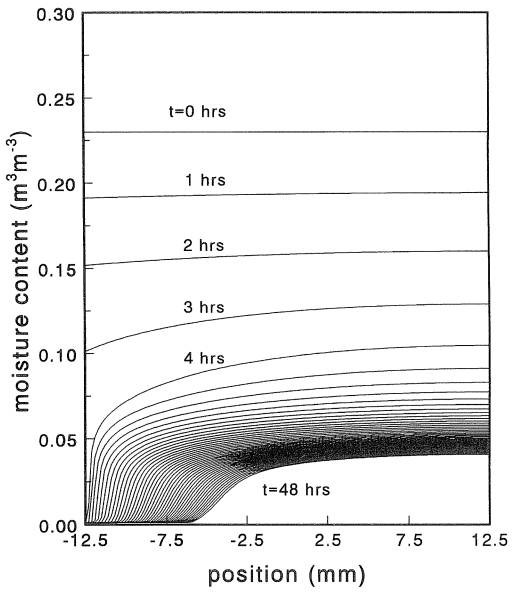

Fig. 8. A computer simulation of the moisture profiles during drying of fired-clay brick (RZ) using the moisture diffusivity plotted in Fig. 7. The time between subsequent profiles is 1 hour and the profiles are given for a period of 48 hours.

The moisture diffusivity for drying over the full moisture content range for the two materials can be obtained by combining the moisture diffusivities found from the moisture profiles during drying and during absorption, with those obtained from the receding front method. The results of such an approach are presented in Fig. 7. Finally, in Fig. 8 a computer simulation of the experiment is plotted for fired-clay brick, using the behaviour of the moisture diffusivity given in Fig. 7.
As expected, the simulated moisture profiles reproduce the experimental profiles given in Fig. 4 very well, except for the first few profiles, indicating that the initial drying rate is underestimated. This may be related to temperature effects.

5 Moisture transport at the brick/mortar interface

In the previous sections attention was given to the moisture transport in various building materials separately. In masonry, however, brick and mortar are bonded. Almost no research has been reported on moisture transport across the brick/mortar interface. Often it is assumed that a perfect hydraulic contact exists between mortar and brick (e.g., Garrecht, 1992). In order to verify this assumption, preliminary absorption experiments were performed on brick/mortar samples.
The cylindrical samples were made up of 110 mm of fired-clay brick and 45 mm of mortar. (The mortar had a cement:sand ratio of 1:4.5 (V/V)). The samples therefore differ from the mortar joints in practice, which have a thickness of the order of 12 mm. A larger mortar "joint" was chosen because of experimental limitations.
The water absorption of each sample was measured from brick to mortar and the opposite, from mortar to brick. In Fig. 9a & b some typical profiles are presented for mortar without air-entraining agent. The position $x = 0$ corresponds to the absorption surface.
Because of the relatively large moisture diffusivity of the brick in comparison to that of the mortar, two situations can be distinguished. In the case of absorption from brick to mortar, moisture profiles start to develop in the mortar when the water reaches the interface. Since the mortar absorbs water rather slowly, the brick is quickly saturated up to its capillary moisture content. In the case of absorption from mortar to brick, the water is quickly absorbed by the brick when it reaches the interface, and after a few hours an almost stationary moisture profile develops in the mortar.
For the mortar it is found that the profiles no longer collapse on a single curve after Boltzmann transformation, indicating that the moisture diffusivity is dependent upon the position. This variation of the hygric properties with position is probably caused by suction of water out of the mortar into the brick during the bonding process. As a result, particles will be transported to the mortar/brick interface and the mortar becomes more compact near the interface (Groot, 1993).
If, as suggested, a perfect hydraulic contact would exist between brick and mortar, each of the materials should absorb moisture up to its capillary moisture content, if the other material is saturated. However, in the case of brick/mortar it appears that the moisture content of the mortar near the boundary does not reach its capillary moisture content, i.e., $\approx 0.20\ m^3m^{-3}$ (see the water absorption experiment from mortar to brick). It is not clear whether this is due to a jump in suction or to a thin layer at the brick-mortar interface which has become less permeable to moisture flow. Of course, experiments over a more extended period of time have to be performed to verify this point.

Also petrographic analysis has to be performed, as especially this technique can give additional information on the microstructure of the cured samples.

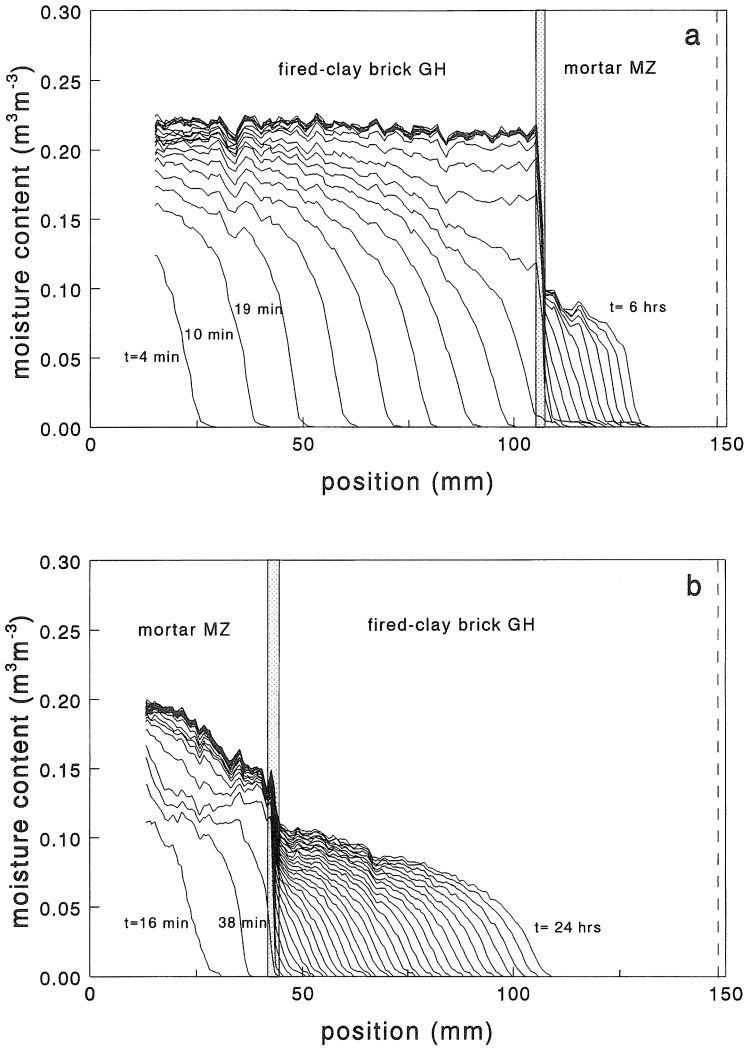

Fig. 9. Moisture profiles measured during the absorption of water in a sample of fired-clay brick (GH) and mortar without air-entraining agent (MZ). The experiment lasted 6 hours in the case of absorption from brick to mortar (a) and 24 hours in the case of absorption from mortar to brick (b). The shaded box indicates the interface area and the dashed line indicates the end of the sample. In figure a 22 profiles are plotted; after the first 10 profiles the time between subsequent profiles is of the order of 20 min. In figure b 34 profiles are plotted; after the first 10 profiles the time between subsequent profiles is of the order of 45 min.

Acknowledgements

The authors wish to thank J. Noyen, H. Smulders and A.W.B. Theuws for their indispensable help in building the equipment and performing the NMR experiments. This project was financially supported by the Royal Association of Dutch Brick Manufactures (KNB).

References

ADAN O.C.G. (1994), *On the fungal defacement of interior finishes,* Ph.D. thesis, Eindhoven University of Technology, The Netherlands.

AMOROSSO G.G. and FASSINA V. (1983), *Stone decay and conservation,* Elsevier, Amsterdam, the Netherlands.

BEAR J. and BACHMAT Y. (1990), *Introduction to modeling of transport phenomena in porous media,* Vol. 4, Kluwer, Dordrecht, the Netherlands.

DIXON R.L. and EKSTRAND K.E. (1982), The physics of proton NMR, *Med. Phys.* **9**, 807-818.

GARRECHT H. (1992), *Porenstukturmodelle für den Feuchtehaushalt van Baustoffen,* Ph.D. thesis, University Karlsruhe, Germany.

GROOT C. (1993), *Effect of water on mortar-brick bond,* Ph.D. thesis, Delft University of Technology, the Netherlands.

KOPINGA K. and PEL L. (1994), One dimensional scanning of moisture in porous materials with NMR, *Rev. Sci. Instrum.* **65**, 3673–3681.

PEL L. (1995), *Moisture transport in porous building materials,* Ph.D. thesis, Eindhoven University of Technology, The Netherlands.

PHILIP J.R. and de VRIES D.A. (1957), Moisture movement in porous materials under temperature gradients, *Trans. Am. Geophys. Un.* **38**, 222–232.

TAMMES E. and VOS B.H. (1984), *Warmte en vochttransport in bouwconstructies,* Kluwer, Deventer, the Netherlands.

WHITAKER S. (1977), Simultaneous heat, mass and momentum transfer in porous media: A theory of drying porous media, *Adv. Heat Transfer* **13**, 119–200.

Notations

B_0	externally applied static magnetic field [T]
D_θ	moisture diffusivity [m^2s^{-1}]
f	frequency [Hz]
RH	relative humidity [%]
x	position [m]
γ	gyromagnetic ratio [MHz/*T*]
θ	volumetric moisture content [m^3m^{-3}]
λ	$= x\, t^{-1/2}$; Boltzmann transformation [$m\, s^{-1/2}$]